# Flight testing delicat – A promise for medium-range clear air turbulence protection

H.P.J. Veerman, P. Vrancken, L. Lombard

▶ **To cite this version:**

H.P.J. Veerman, P. Vrancken, L. Lombard. Flight testing delicat – A promise for medium-range clear air turbulence protection. European 46th SETP and 25th SFTE Symposium, Jun 2014, LUELA, Sweden. hal-01111380

**HAL Id: hal-01111380**
**https://hal.science/hal-01111380**

Submitted on 2 Feb 2015

**HAL** is a multi-disciplinary open access archive for the deposit and dissemination of scientific research documents, whether they are published or not. The documents may come from teaching and research institutions in France or abroad, or from public or private research centers.

L'archive ouverte pluridisciplinaire **HAL**, est destinée au dépôt et à la diffusion de documents scientifiques de niveau recherche, publiés ou non, émanant des établissements d'enseignement et de recherche français ou étrangers, des laboratoires publics ou privés.

# FLIGHT TESTING DELICAT – A PROMISE FOR MEDIUM-RANGE CLEAR AIR TURBULENCE PROTECTION

**Henk P.J. Veerman[1], Patrick Vrancken[2], and Laurent Lombard[3]**

[1] National Aerospace Laboratory, NLR
Anthony Fokkerweg 2, 1059CM Amsterdam, The Netherlands
e-mail: veerman@nlr.nl

[2] Deutsches Zentrum für Luft- und Raumfahrt, DLR
Oberpfaffenhofen, 82234 Weßling, Germany
e-mail: Patrick.Vrancken@dlr.de

[3] Onera - The French Aerospace Lab,
91123 Palaiseau, France
e-mail: Laurent.Lombard@onera.fr

**Abstract**
Atmospheric turbulence encounters are a major cause of injuries to passengers and flight crew in non-fatal airline accidents. A whole class of turbulence, representing 40% of turbulence accidents and designated as Clear Air Turbulence, cannot be detected by any existing airborne equipment, including state-of-the-art weather radar. Also the number of turbulence accidents has been growing since 1980, 3 times faster than the increase of air traffic.
Flight operational concepts for protection against turbulence hazards include:

- Short range (50 m to 300 m) measurement of air speed ahead of the aircraft and action on the aircraft flight controls to mitigate the effect of turbulence
- Medium range (10 km to 30 km) detection of turbulence and securing of passengers and crew members by seat belts fasten or other mitigation

Both concepts could be supported by UV LIDAR technology. The objective of DELICAT was to validate the concept of LIDAR-based medium-range turbulence detection.
Within the EC FP7 project DELICAT a UV LIDAR system was designed and manufactured for application in airborne environment by a European consortium consisting of industrial partners, research institutes and universities. First the LIDAR was laboratory tested and ground tested scanning the atmosphere. Subsequently, it was installed in NLR's Cessna Citation research aircraft and flight tested in atmospheric conditions from non-turbulence up to medium-turbulent level. During the flight tests the atmosphere was analysed by the UV LIDAR in combination with aircraft on-board sensors. The collected data from aircraft sensors vs. LIDAR were compared after the flight. The correspondence between LIDAR backscattered energy fluctuations and turbulence experienced by the aircraft, for a given atmosphere volume was evaluated. The paper will discuss the flight test techniques needed for the project, i.e. a description of the instrument evaluated, installation of the instrumentation in the aircraft, the flight test plan, the execution of the flight test campaign, the measurement results and the flight test lessons learnt.
During the project challenges of various kinds were met. A heavy, powerful laser had to be installed into the aircraft cabin without compromising cabin and airspace safety. Also aircraft external modifications were made, such as vanes attached to a nose boom measuring airflow, a fairing enabling guidance of the laser beam from cabin into airspace ahead of the aircraft,

exchange of standard cabin windows with dummy windows with inserts, mounting of a fast temperature probe, etc. The aircraft modifications required approval by the Dutch CAA leading to a Supplemental Type Certificate. Other challenges were design and aircraft integration of a beam steering system enabling the laser beam to be directed into the flight direction of the aircraft whatever its attitude. Key to success was finally finding enough turbulence encounters. This was realized in cooperation with European meteorological organizations Meteo France and ICM from Poland forecasting promising areas and time slots in European airspace.

In total about 40 hours of flight testing were executed in European airspace in which events of clear air turbulence were encountered. This enabled the team to demonstrate the working principle of the system. Further analysis of collected data is to confirm that LIDAR technology can indeed detect clear air turbulence kilometres ahead of the aircraft.

## 1 INTRODUCTION

Atmospheric turbulence encounters are the leading cause of injuries to passengers and flight crews in non-fatal airline accidents. Federal Aviation Administration (FAA, US) statistics show an average of 58 airline passengers are hurt in U.S. turbulence incidents each year (from NASA press release n°04-035, 08/06/2004). Figure 1 indicates that the number of accidents is increasing, due to traffic and load factors increasing (extracted from [1]). The corresponding cost is estimated over US$100M per year for commercial airlines in the US alone. The situation may even worsen in future years, because new aircraft are being designed to allow passengers to circulate freely for entertainment and exercise during long-haul flights.

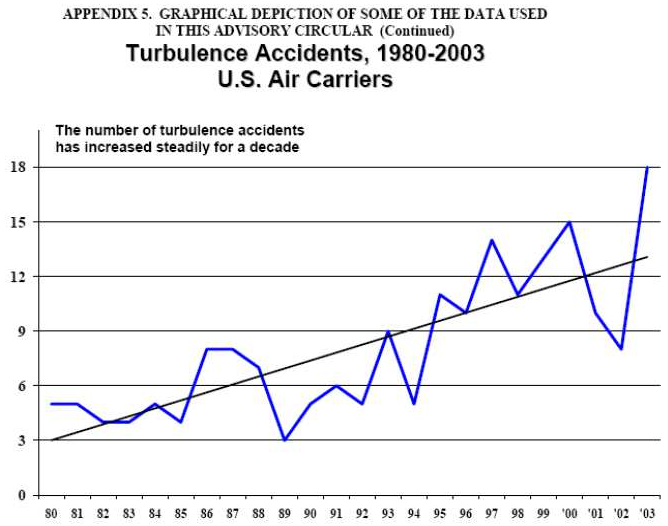


Figure 1: Evolution of turbulence accidents for US air carriers, 1980 - 2003

Distinction can be made on the one hand on the turbulence kind and source and related with it the airborne sensing capabilities and on the other hand the range to the turbulence area and associated with it the possible mitigation actions.

In [1] the following turbulence classification is presented:

- **Clear Air Turbulence (CAT)**. In general this is high altitude turbulence (above 15000 ft.) not normally associated with cumuliform cloudiness, however generally occurring in the neighbourhood of jet streams. It can be characterised as typically wind shear induced turbulence.
- **Mountain Wave Turbulence (MWT).** This is turbulence as a result of strong winds

blowing over a mountain range or a sharp bluff, causing a series of up-drafts and downdrafts after passing the range.

- **Convectively-Induced Turbulence (CIT)**. In general, the development of a thunderstorm will generate oscillations in the stable and clear atmosphere above and even up to hundreds of miles of it.

Of these three categories of turbulence state of the art weather radars are able to detect thunderstorm that may generate turbulence above and around itself. The weather radar cannot detect CAT where neither rain droplets nor hail is present. Thus, the weather radar cannot protect the aircraft neither in case of Shear Induced Turbulence, nor in case of Mountain Wave Turbulence. The fact that shear induced CAT cannot be detected by weather radar explains that although weather radars have been used on board all commercial aircraft for many years, the number of accidents caused by turbulence is still increasing.

Turbulence categorized by range to the aircraft and associated operational concepts can be categorized as follows:

- Long range: distance > 30 km, time > 2 minutes. Operational concept is to avoid turbulence encounters based on meteo information. Detection capabilities are not foreseen in the near future.
- Medium range: distance 8 to 30 km, time 30 s – 2 minutes. Operational concept is to detect turbulence above severity threshold including time to encounter, followed by passenger and crew protection by seats belt fasten.
- Short range: distance 50 – 300 meter, time 0.2 – 1 second. Operational concept is to protect passengers, crew and aircraft by mitigation of the turbulence effects by flight controls.

The DELICAT (DEmonstration of LIdar based Clear Air Turbulence detection) project aimed at identifying if LIDAR could be a solution for sensing (and subsequently protecting) against medium range turbulence that cannot be sensed by weather radar, i.e. detecting medium range CAT at distances of at least 10 km.

Figure 2: Kelvin-Helmholtz clouds indicating shear induced turbulence conditions

## 2 OBJECTIVES OF DELICAT

From earlier experiments, e.g. in European Framework projects (FP6) [4] and earlier it is known that a LIDAR sensor is capable of detecting turbulence. LIDAR stands for LIght Detection And Ranging, whereas RADAR stands for RAdio Detection And Ranging. The basic difference between a LIDAR and a Radar system is that optical wavelengths in the ultraviolet,

visible, infrared parts of the electromagnetic spectrum are used, instead of radio frequencies. Since the wavelength used by a LIDAR is much smaller than the one used by the Radar (by a factor of $10^{-4}$ to $10^{-5}$), the LIDAR can "see" much smaller objects than the radar, for example air molecules ($N_2$ or $O_2$) or aerosols. Thus the LIDAR is well suited to analyze the clear atmosphere surrounding an aircraft. The LIDAR uses the properties of the backscattered light to obtain information on a distant target or on the atmosphere. The knowledge of the exact position of the portion of atmosphere under analysis with respect to the light emission can be obtained using the time of flight between emission and reception of the signal. Physical principles of the method are described more in-depth in the next chapter.

DELICAT will validate LIDAR as an advanced and new technology for medium-range detection of CAT at >10 km distance ahead of the aircraft allowing efficient protection of passengers and crew by taking appropriate actions inside the cabin (fasten seat belts, fixing objects, etc.). This technology, combined in single equipment performing both-short range and medium-range turbulence protection, may in future provide a very efficient turbulence protection system for passengers and crewmembers.

About 30% to 40% of turbulence accidents are not directly linked to convective phenomena (e.g. thunderstorms), and so cannot be detected even by state of the art weather radar. Contrary, those accidents could be avoided by the use of this UV LIDAR turbulence protection equipment, which would then allow for a reduction of the number of turbulence accidents roughly by the same factor (30% to 40%).

In the DELICAT project, the validation of medium range turbulence detection will be based on the comparison of the information on a turbulent atmospheric area, provided on one side by remotely back scattered light of a UV LIDAR and on the other side by the aircraft sensors, i.e. Inertial and AirData Systems, measuring as a reference accelerations, air speed and temperature variation. This experiment thus uses the aircraft as an 'in-situ' truth sensor when the turbulence area is reached and will allow a solid assessment of the performances of the UV LIDAR detection technology, including False Alarm Rate and Missed Alarm Rate. The LIDAR system will include all the basic functionalities of future medium range detection LIDAR equipment, even though those functionalities will have a lower maturity level (for example, in DELICAT signal processing will be performed off line instead of in real time).

Apart from this primary objective, secondary induced objectives can be identified as well. As moderate and severe turbulence area encounters are in general rare, odds for turbulence encounters must be enhanced by cooperation with meteo service providers. This increase in turbulence encounters can be obtained together with meteo service providers by:

- Selecting the turbulence phenomena that are most promising to encounter;
- Selection of the most favorable location and time (strategic flight campaign planning);
- Short term or even real-time support to flight tests (tactical support).

In return, the analysis of the LIDAR and aircraft sensor data collected during the flight tests and their comparison with forecasting situations will allow improving the understanding of CAT inducing atmospheric phenomena and also improving the CAT forecasting capabilities of European meteo services providers. This knowledge could result in optimized CAT-safe flight plans and optimum 4-D aircraft trajectories.

## 3 PHYSICAL PRINCIPLES OF LIDAR BASED TURBULENCE DETECTION

As identified in the introduction clear air turbulence can be associated with two atmospheric mechanisms: gravity waves in the lee of orography (mountain waves) and jet stream induced turbulences [3]. Turbulence is the result of large, unexpected and non-stationary vertical velocities of air, both upward and downward. When the scale (in term of dimension or time) of these vertical velocities variations lie within the aircraft sensitivity bandwidth, this results in large vertical and lateral accelerations, sometimes larger than 1 g. The inhomogeneous structures of these velocities may also induce large changes in the attitude of the airplane.

At medium range (more than a few km), vertical velocities cannot be directly measured by the Doppler shift of a radiation (whatever the wavelength), because the movement is perpendicular to the Line Of Sight (LOS) and so produces no Doppler shift.

However, the studies conducted in the frame of the DETAC (French DPAC project) and FLYSAFE (FP6) [4] have shown that indirect turbulence detection can be achieved through the measurement of air density fluctuations, with direct relationship between density fluctuations and vertical air velocity:

$$\delta\rho/\rho = (N/g)\, w$$

where is $\rho$ the density, g the gravity acceleration, w the vertical air speed, and N the Brunt-Väisälä angular frequency (N quantifies the atmosphere thermodynamic stability and is positive for stably stratified atmosphere).

This relationship comes from calculations taking into account both linear (gravity waves) and non-linear situations, resulting from the conditions of appearance of turbulence. More details can be found in the Final Report of the FP6 FLYSAFE project [4]. According to this relationship a local vertical gust of amplitude w, possible origin of turbulence sensed by the aircraft, will also result in a local variation of the air density $\delta\rho/\rho$.

Although Doppler shift cannot be used for turbulence detection based on LIDAR back scatter, other properties of the back scattered light may be used to analyze the atmosphere. The atmosphere has two main elastic backscatter mechanisms that may be used for analysis:

- Mie backscatter, corresponding to the aerosols or other particles, whose size is of the order of that of the wavelength or greater. The energy of the Mie backscatter signal is proportional to the concentration of aerosols. The spectral bandwidth of the Mie backscatter is narrow, similar to that of the laser,

- Rayleigh backscatter, corresponding to the molecules (mainly the molecules of nitrogen and oxygen). The energy of the Rayleigh backscatter is proportional to the atmosphere density. The spectral bandwidth of the Rayleigh backscatter is relatively broad, due to the random Brownian movements of the air molecules (at a speed close to the speed of sound)

The energy of the Rayleigh backscatter is proportional to the air density, and thus a possible local air density fluctuation, linked to a vertical gust, will be detected through the analysis of the Rayleigh backscattered energy, corresponding to the molecules backscattering (see Figure 3). Mie backscatter is a source of noise to be filtered out.

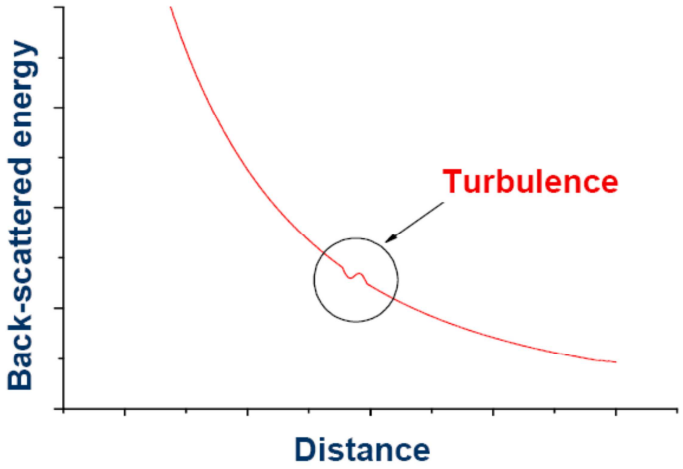


Figure 3: Principle of a LIDAR based turbulence detection (without noise, the shown turbulence effect being greatly exaggerated and simplified)

## 4 LIDAR DESIGN AND FUNCTIONALITY

A lidar is generally composed of two main elements: A laser transmitter emitting laser radiation into the atmosphere and a receiving system that collects and detects the backscattered radiation. For DELICAT, a special beam steering system has been added in order to direct the laser beam into the flight path, i.e. that the aircraft is actually flying into the region firstly sounded by the lidar.
As described above, the DELICAT lidar is sounding the atmosphere ahead of the aircraft for local variations in air density by analysing the backscattered light intensity:

$$\frac{\Delta\beta_{Ray}}{\beta_{Ray}} = \frac{\Delta\rho}{\rho} = w\frac{N}{g}$$

Where $\beta_{Ray}$ is the backscatter coefficient of air (Rayleigh process) at the respective wavelength, $\rho$ the air density, w the vertical wind speed (as a measure for the turbulence strength), N the Brunt-Väisälä frequency (with typical values between 0.01 to 0.02 rad/s) and g the gravitational acceleration.
For typical turbulence the molecular density fluctuation is thus on the ~1% level.
In order to achieve this level, the lidar is designed and operated the following way: The transmitter is emitting UV (ultraviolet) laser pulses in the atmosphere which ensures a high backscatter coefficient (as opposed to infrared radiation, e.g.) from the air molecules ($N_2$ and $O_2$ mainly) since the molecular backscatter cross section has a $1/\lambda^4$ dependence. Another advantage is the less (but still) critical issue for eye safety as opposed to the visible region.
On the receiver side, a large number of lidar signals is averaged in order to decrease the noise below the turbulence detection limit. For within the DELICAT project, the minimum requirements for the concept demonstration have been set to: 1% density fluctuation at 5km detection distance.
The molecular density backscatter fluctuation can be polluted by the aerosols density fluctuation, which are not expected to be related to the presence of turbulence. Fortunately, amount of aerosol is very low at chosen flight level. Furthermore, most kinds of aerosols at this altitude (in particular ice crystals) depolarize backscattered light while molecules do not. A polarization analysis will then allow to discriminate areas polluted by depolarizing aerosols.

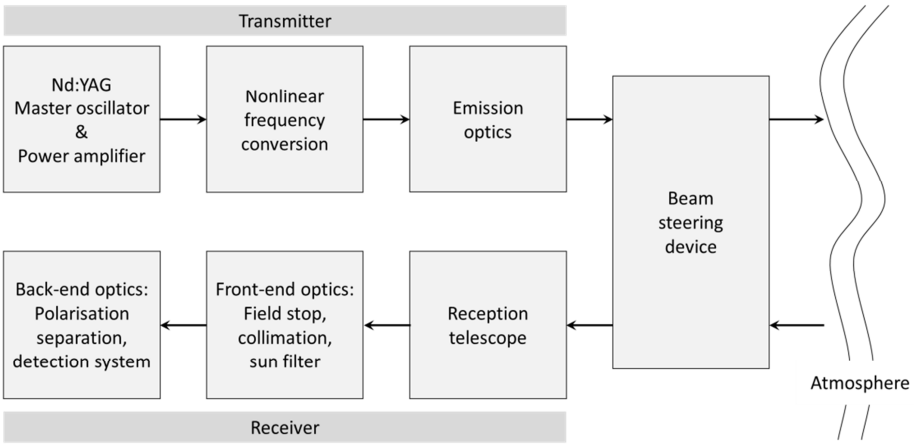


Figure 4: Synopsis of the DELICAT lidar system

The following sections describe the lidar system, developed, manufactured and operated by DLR in more detail.

### 4.1 Lidar transmitter

The DELICAT transmitter is based on a high-power Nd:YAG laser issued from the DLR water vapour DIAL (differential absorption) lidar WALES [5].

The laser is of the MOPA (master oscillator – power amplifier) design, with a monolithic Nd:YAG ring laser as master that runs intrinsically single-mode. It emits IR (1064 nm) laser pulses at a rate of 4 kHz and a pulse length of 7.7 ns (FWHM). A part of the laser pulses (at a rate of 100 Hz) is amplified in three power amplifiers, one in double-pass, and two in single-pass. The resulting energy per pulse is then $\geq$ 400 mJ.

The infrared laser pulses are then transformed into UV radiation by a non-linear frequency conversion. Thus, they are fed into a KTP crystal (Potassium titanyl phosphate) for second harmonic generation, i.e. conversion into visible/green radiation at 532 nm. Subsequently, the generated green and the residual IR radiation are guided into a BBO crystal (Beta barium borate) for sum-frequency generation. The resulting 355 nm laser pulses then have an energy of ~80 mJ. Part of the beam is sampled and directed onto a photodiode to monitor the pulse-to-pulse energy.

The residual infrared and green radiation is separated from the UV by a set of dichroic mirrors and fed onto a dump. By this means, practically only UV light is emitted by the transmitter system.

The following image depicts the high-power transmitter. The rear red box contains the IR MOPA part of the laser, and the pink front the THG (third harmonic generation) stage. While the upper part contains all laser optics, the lower half of the system contains all power and control electronics. The intermediate base houses a water-based cooling circuit for the chilling of the high-power laser rods and electronics.

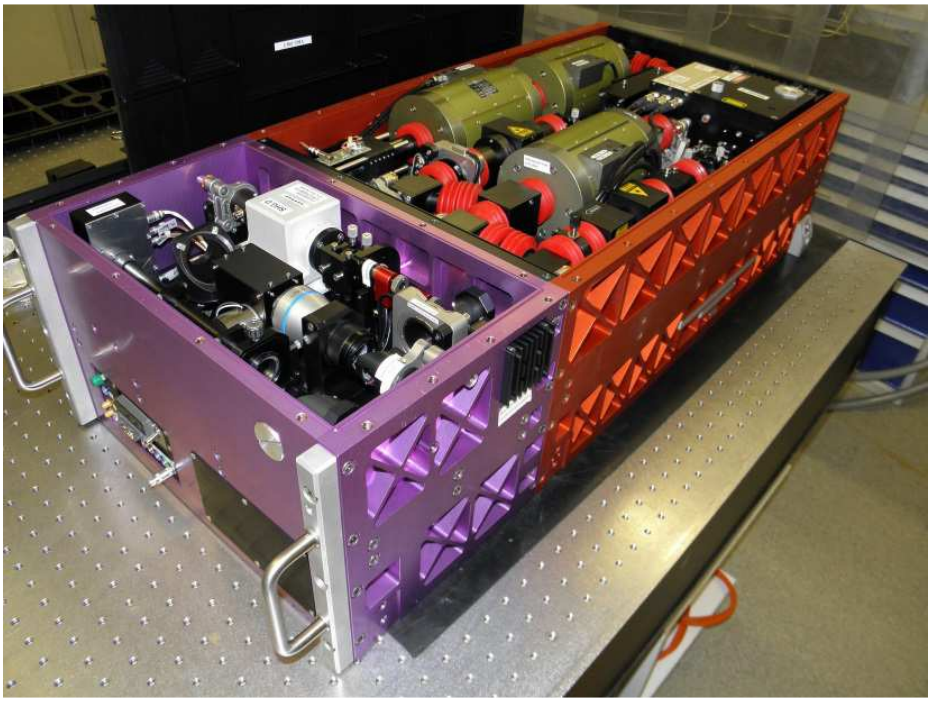

Figure 5: The DLR lidar transmitter with THG (front) and IR high power laser (rear)

The output laser beam is then expanded to a diameter of ~15 mm while meeting a divergence of 200 µrad. A beam feed then guides this high-power laser beam to the transmit mirror which is co-aligned with receiver's system secondary telescope mirror (monostatic arrangement, i.e. the emission direction is concentric with the reception direction).
Both the transmission and the receiving 'beams' commonly use the beam steering optics (third section).

### 4.2 Lidar receiver

The DELICAT lidar receiver consists of the main modular subsystems: telescope for efficient light collection, front optics for filtering and beam forming and back end optics for detection. It allows a versatile use (as in this project) while being adaptable to further evolution.
The telescope is of the Newtonian (Ø = 6", F/5) architecture allowing for a small secondary and flat mirror. The used diameter of 140 mm is defined by the restriction of the fairing front window aperture. The front-end contains a field stop in the telescope focus defining a FOV (field of view) of 1 mrad allowing for alignment errors and possible vibration effects of the 200 µrad laser beam within the FOV.
A collimation optic then generates a parallel beam of some mm diameter which is fed through a narrow interference filter (0.5 nm, peak transmission ≥ 80 %) for the blocking of solar background.

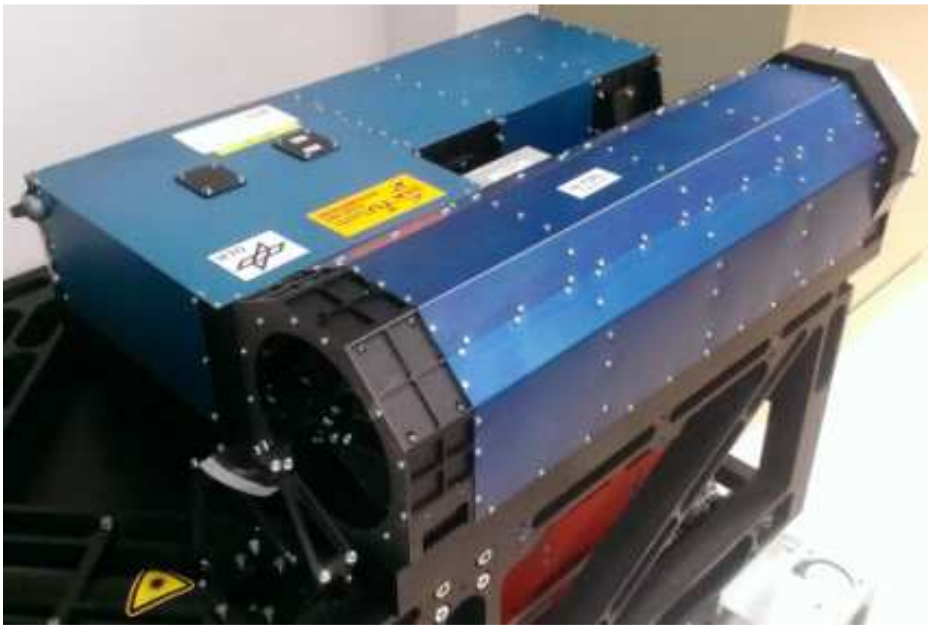

Figure 6: The DLR receiver system

The receiver back-end then features a polarisation separation assembly allowing the separation of the backscattered radiation with perpendicular polarisation to the emitted one from the parallel one. Both channels are then fed onto PMT (photo multiplier tube) detector modules.
The polarisation separation is one half of the double strategy to aim for the molecular (i.e. density) signal (which does barely depolarise) only, while not being disturbed by any aerosol backscatter. Since the depolarisation can only give an indication on the presence of aerosols (since not all aerosols feature depolarisation, as for instance spherical particles as haze and soot and if, not a constant value), the second half of the strategy is to perform the flight tests within areas forecasted to be aerosol devoid (or with low concentration). This is achieved by a forecast from the DELICAT meteo partners and a study on the aerosol backscatter statistics in the UV with respect to mass ratio.
The two polarisation detection channels (parallel, i.e. molecular, and perpendicular) are composed of the DLR WALES detection modules which consists in a PMT, high voltage supply and early digitising, all integrated into a single box.
The PMTs' digitised signals feature a sample rate of 30 MHz which results in a lidar range resolution of 5 m. The data acquisition runs continuously and thus also registers the sun-generated background signal which is then subtracted in the signal post-processing. The DLR data acquisition thus stores (for the DELICAT purposes) one lidar signal with a 15 km range per laser shot (at a rate of 100 Hz) resulting in the considerable data amount of more than 10 Gb/h.
The data acquisition system further controls the transmitter operation and features a GUI (graphical user interface) for the operator in order to control all lidar functionalities.

### 4.3 Beam steering system

The DELICAT beam steering system is an example of very successful joint development between three different partners. While the overall system has been designed and built by Thales Avionics, it features many, partly interleaved interfaces with both NLR and DLR systems. So does it use NLR ARINC data for its control and has direct mechanical interfaces to the aircraft (fuselage) and further has mechanical and optical interfaces to the DLR lidar rack (see below) and to the windows also supplied by DLR. The development work was marked by a number of iterations in the domains of mechanics, optics and data also employing different

modelling software such as CATIA for the mechanics and ZEMAX for optical layout. The following section briefly describes the system.
The main requirement of the beam steering system is to maintain the lidar transmit/receive beam parallel to the flight path while the aircraft changes its attitude: Change of angle of attack due to decreasing weight, residual movements of the autopilot and light turbulence with a identified bandwidth.
An important feature is however that the receive beam (Ø 140 mm) should not be further truncated by that movement which may only be achieved by making it invariant at the exit (i.e. fairing window). This results in the need of a set of two movable mirrors (a reflective scanning system architecture has been chosen for economic and UV compatibility reasons). Both are two-axes movable and controlled in real-time by a unit which gathers its data from the aircraft ARINC stream containing the appropriate attitude (IRS) and flow (nose boom vanes) angles.

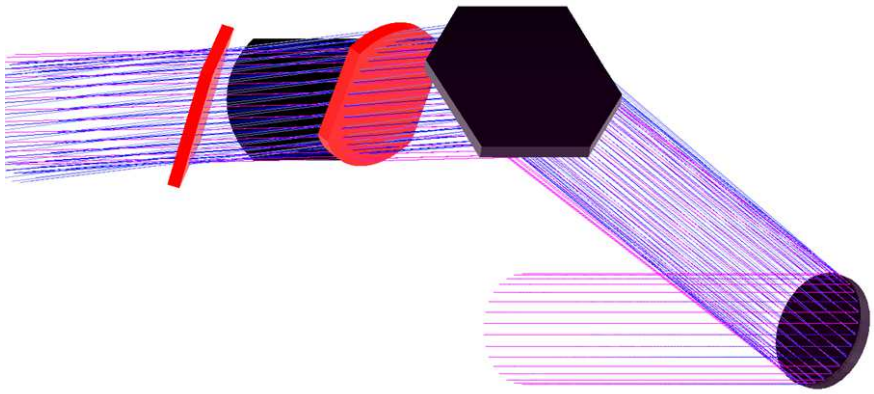

Figure 7: A ZEMAX simulation of the lidar receive 'beam' transmitting through and over the different optical elements (by Thales Avionics). From upper left to lower right: Fairing window, outer bending mirror, cabin window, 2nd beam steering mirror, 1st beam steering mirror. In the lower central part would be located the lidar receiver telescope.

A third, fixed mirror is located on the aircraft outside, inside the protective fairing. The laser beam thus travels over the two movable beam steering mirrors, through the UV-Quartz window (replacing the standard window), over the outer mirror, which bends the beam into forward direction, and though the fairing front window (also UV-Quartz).

### 4.4 Lidar mechanical integration

The whole lidar system consisting of transmitter, receiver and beam steering mirrors plus monitor and further accessories is mounted into a stiff (optical constraints) and rugged (airworthiness constraints) rack structure as may be seen on the following image.

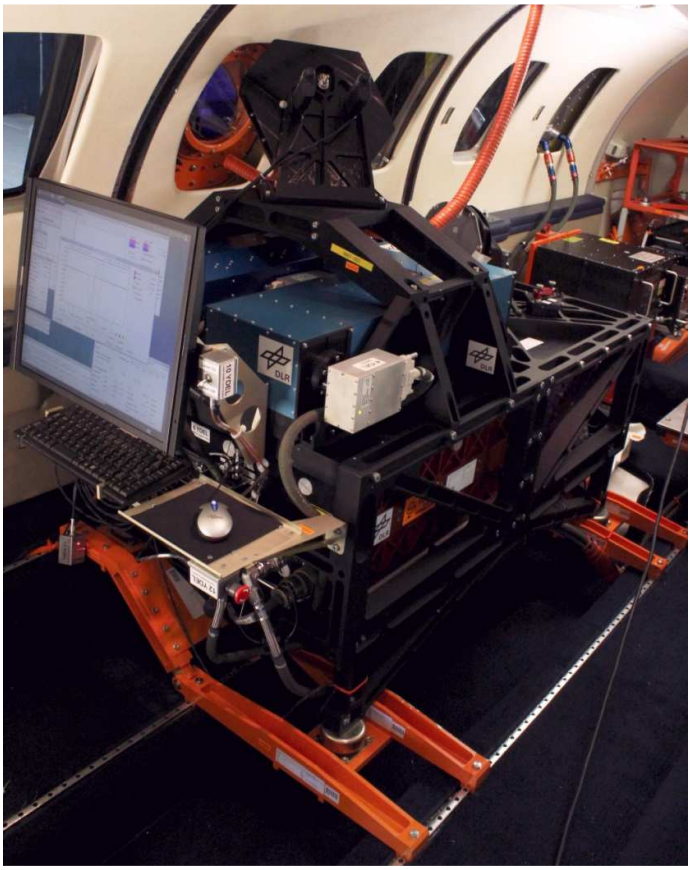

Figure 8: The DLR lidar system with Thales beam steering system, mounted to the Citation seat rails

## 5 AIRCRAFT MODIFICATIONS AND SYSTEM INTEGRATIONS

Apart from the LIDAR system itself, various systems had to be integrated into the aircraft cabin, either to support the LIDAR or to serve as a reference system to verify performance of the LIDAR. In addition to these system integrations, various modifications to the Citation aircraft had to be made, making the complete picture of adaptations quite significant and complex.

Figure 9: DELICAT equipment installed inside cabin of Cessna Citation II

### 5.1 LIDAR Related Aircraft Modifications

In order to obtain the measuring accuracy that was required for the tests the LIDAR was housed in a rigid rack together with two steering mirrors and mounted upon the seat rails at both sides of the cabin in order to reduce loads. For mounting the 240 kg heavy LIDAR rack a newly designed mounting provision was used (see Figure 10).

Figure 10: Empty LIDAR rack mounted upon seat rails

The UV light needed to be transmitted undisturbedly into the heading direction of the aircraft. For this purpose the standard cabin window had to be replaced by an optical window that was transparent in the UV part of the spectrum. This UV optical window was supported with a fixed mirror reflecting the exiting LIDAR light into forward direction. The optical window with mounted forward bending mirror was housed inside a fairing specifically designed at NLR for accommodating fuselage-external equipment. The powerful LIDAR transmitter is producing significant heat of ~1 kW. This heat must be dissipated by a cooling system, keeping the laser at the right temperature. This cooling system would rise the cabin's temperature to unacceptable levels when its heat would be released inside the cabin. As a solution the two-circuit cooling system (water/oil) was equipped with a finned cooler plate through which cooler liquid was flowing that was replacing another cabin window. In this way excess heat was directly released to the aircraft exterior, using the atmosphere's air flow and low temperatures.

Figure 11: UV optical window with mounted forward reflecting mirror

In order to test the LIDAR performance by using the aircraft as a turbulence reference sensor, the LIDAR beam had to point right into the aircraft's heading direction with 0.1° accuracy. For enabling this pointing accuracy various supporting equipment was involved. To start with, the two bending mirrors on top of the LIDAR rack were equipped with actuators enabling the LIDAR system to react to the aircraft's attitude variations, e.g. as a result of fuel consumption or local variations in wind speed. Both mirror actuators were controlled by a Beam Steering System. The information on the parameters that influenced the LIDAR pointing direction needed to be fed real-time into the Beam Steering System. For this purpose an Inertial Reference System (IRS) measured the aircraft's attitude and heading, while vanes mounted on a nose boom measured the aircraft's angle of attack and angle of sideslip relative to the surrounding air flow. It was required to fly the aircraft with 1.25° side slip angle in order to avoid partly occultation of the back scattered LIDAR beam by the fuselage of the Citation. All information from aircraft sensors to the beam steering system were exchanged as Arinc 429 data samples and distributed via the Datalogger system that also recorded all sensor data (except from the LIDAR) for later analysis. All systems were synchronized at 1 ms timing accuracy based on a GPS slaved clock.

Figure 12: Modified Citation including nose boom and fairing

### 5.2 LIDAR Reference Systems

The aircraft itself was used as reference for the performance measurement of the LIDAR: in case the LIDAR receiver measures distant turbulence, the aircraft was used to confirm this measurement, assuming that the remote atmospheric turbulence conditions did not change too

much in few minutes time lapse. For this reference purpose the IRS was used, measuring aircraft's accelerations in three components X, Y and Z at 50 Hz. It was also expected that the nose boom vanes would measure turbulent flow conditions. Because of the fact that local temperature variations are expected in turbulent air masses as a result of adiabatic compression and de-compression a high speed (0.1 second relaxation time) high accuracy (0.1°C relative temperature) Total Air Temperature (TAT) probe, specifically designed for flight testing, was mounted at the fuselage. This latter sensor was included to the test, because it was of specific interest from atmospheric research perspective.

## 6 CERTIFICATION ISSUES

In recent years requirements for certification of aircraft modifications have increased considerably. For being approved to fly the modified Cessna Citation II a Supplemental Type Certificate (STC) had to be obtained. This STC request was issued to IL&T, the Dutch CAA after considerable efforts and obtained on July 16th, 2013 after which the flight test campaign was commenced. Certifications issues for approval of aircraft modifications were diverse and had to be proved by various tests. Most important topics were related with cabin safety, aerodynamics and flight operations. For facilitating the certification process NLR has implemented a 'Research Aircraft Design Organization' (RADO).

Concerning aerodynamic tests the first approval tests started already 2010, when an RVSM certificate (Reduced Vertical Separation Minima) was obtained for the Citation including both nose boom and fairing. This certificate must be obtained because the flight tests are anticipated to be executed in upper airspace (above FL290), where jet stream related turbulence is expected. Due to nose boom and fairing mounting it must be proved that the PEC (Position Error Correction) of the modified aircraft was within margins relative to the certified clean configuration. In a flight test it was shown that no significant effects on the Air Data Computer were measured. The fairing was already designed and approved for an earlier project, however these former flight trials were executed under atmospheric, non-pressurized conditions and at low MACH numbers, which were not the case for the DELICAT trials. In a CFD assessment the aerodynamic effects of the fairing on the flow was investigated. It showed that effects of the fairing were acceptable, especially concerning flow changes near the engine inlet. A FEM analysis showed that structural load on the fairing mounting due to expansion of the pressurized cabin was too high. A solution was found in changing mounting provisions: four connectors were replaced with sheer tolerant fasteners. Finally a certification flight prior to the test campaign showed that indeed no influence on engine thrust was noticed while the fins on the cooler plate did not introduce noticeable increase of noise.

Concerning cabin safety, the most critical issues were related with loads related with installation of the 240 kg LIDAR rack upon the seat rails, operation of a dangerous class 4 UV laser inside the cabin, the instrumentation volume (free way to emergency exit and free way to fire source), safety of the optical glass window and use of a nitrogen bottle for drying air inside fairing to avoid condensation on glass surfaces. In a FEM analysis it was shown that loads by the LIDAR rack on the seat rail mounting locations did not exceed the standard load introduced by a passenger-seat combination. Compliance with free way requirements was shown in evacuation tests. The cabin was made laser safe by using a curtain covering the LIDAR. The intended laser safety curtain did not pass the flammability tests marginally. A CRI (Certification Review Item) based solution was not accepted by CAA. Finally a fire extinguishing blanket was tested successfully, both meeting UV opacity and flammability requirements. In addition to a laser safety curtain UV protecting goggles were used by the flight crew in case the curtain had to be removed, e.g. for laser adjustments. The strength of the UV glass re-

placement was an essential part of the cabin safety approval. First DLR made a theoretical assessment on glass strength properties. This analysis was input to the design of the optical glass window, defining the minimum thickness of the glass plate. Subsequently the UV transmitting glass plate was sustenance tested at a climate chamber: inside the chamber atmospheric low pressure low temperature conditions were simulated, while outside the climate chamber the ambient cabin conditions were simulated. The glass plate was tested on a number of flight cycle simulations, an endurance test and an ultimate load test. These glass strength tests were witnessed and approved by an agent of the Dutch CAA. Use of a nitrogen bottle could not be certified, therefore this system was abandoned. Instead, the fairing was filled with nitrogen at the airfield prior to the flight, which proved adequate.

Flight operation certification issues were addressed in two documents. As part of the Flight Test Plan an analysis was made of all possible hazard situation including mitigation actions when needed. Also an Aircraft Flight Manual supplement (AFM-supplement) was made defining all additional operational safety measures, including

- Defined flight conditions;
- Use of laser emergency stop;
- Physical angle restrictions;
- ATM related safety measures, concerning use of class 4 laser in airspace

## 7 SYSTEMS CALIBRATIONS

In order to really obtain a LIDAR pointing accuracy of at least 0.1° all involved systems need to be carefully aligned. Thus the aircraft fuselage alignment with the seat rails, IRS orientation, nose boom and LIDAR beam were carefully calibrated. These calibrations combined and resulted into calibration offsets and factors that were defined in the Beam Steering System. For adequate alignment of these systems a number of calibrations were needed. For calibrating the attitude of the vanes with the synchrometer that senses the vanes rotation a special nulling device was designed. It was shown that this vane-synchrometer combination showed no noticeable hysteresis. Alignment of aircraft nose boom and the transmitter beam was conducted inside the hangar using a laser-based waterlevel. In this way the mirror actuators zero positions and rotation matrices for actuator commands of the Beam Steering System could be determined.

Alignment of the Citation fuselage with IRS and nose boom vanes was performed at the apron. For this alignment a tower with known position at 12.67 km distance in the city Haarlem was used. While moving the aircraft the tower's peak was positioned at the hair cross at the centre of a visor that was attached to the nose boom (see Figure 13). Thus a measurement accuracy of 0.04° was obtained.

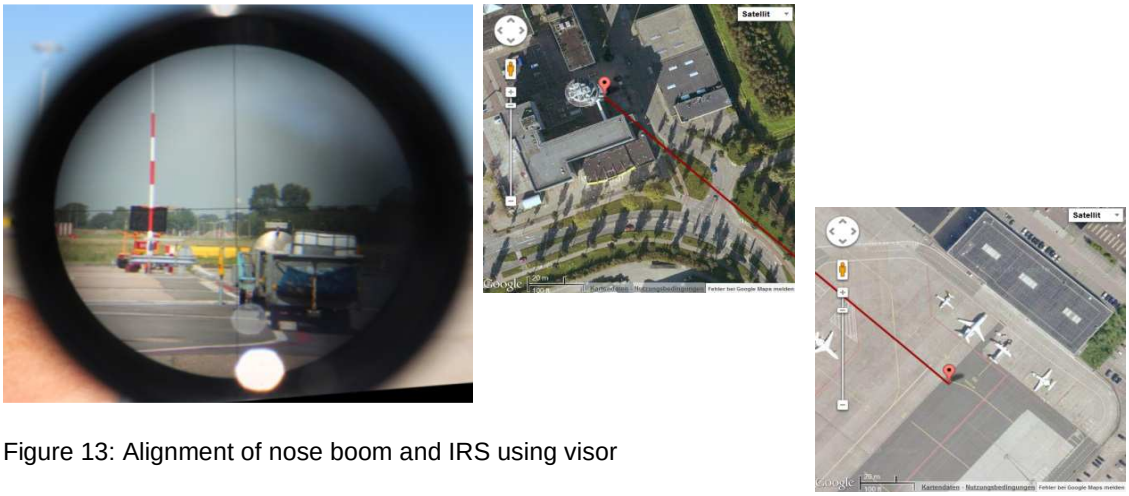


Figure 13: Alignment of nose boom and IRS using visor

A final calibration that needed to be performed was concerning the vanes rotation correction factor that results from aerodynamic interference (see Figure 14). As a result of boom self-induced and airframe induced flow distortions a correction factor on the vane rotations must be applied. The value of this factor is a function of airspeed and flight altitude (or air pressure), however can be considered as a constant when speed and flight altitude will be kept approximately at constant value. The value of this flow distortion correction factor was calculated based on CFD analysis and verified with a special flight pattern (clover leaf, nulling out any crosswind). To enable the CFD analysis the 3D shape of the Citation's fuselage and nose boom was scanned using a laser scanner. The flow distortion at the location of the centre of the β-vane assembly (the most important vane for DELICAT) was determined leading to the applicable value of the flow distortion correction factor. The CFD-calculated value of the correction factor was further confirmed later, in another project after the DELICAT flight trials.

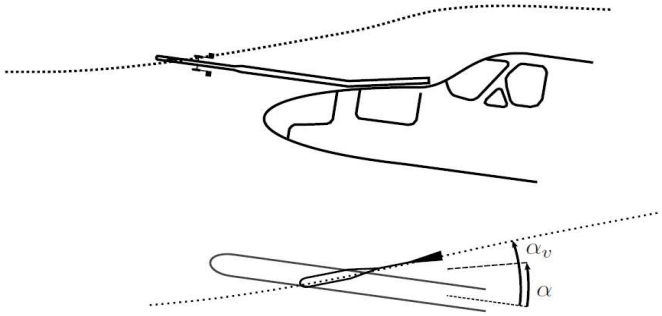


Figure 14: Airframe induced flow distortion at vane location

## 8 FLIGHT TEST CAMPAIGN

Shortly after the STC was obtained the DELICAT flight test campaign was started. The campaign started with a short shakedown flight in which the correct operation of all involved systems was proved under airborne conditions. Subsequently in the period July 17th 2013 until August 13th, 2013 the flight test campaign was active. Every day in this time period started with a teleconference between meteo service providers Meteo France and ICM from Poland and the flight crew, consisting of the pilots, LIDAR operator (DLR) and a Flight Test Instrumentation Engineer (FTIE) from NLR. On several days also a second, afternoon meteo teleconference was held. In these teleconferences it was decided if nearby favourable CAT conditions could be found, or if at more remote distance CAT conditions could be found during a period of more than one day. In case it was worthwhile to start a flight test on that day or on the next day the optimal trajectory for finding moderate CAT conditions was determined, subsequently a flight plan was issued. Severe CAT conditions were to be avoided, although such

conditions were not prevalent in the flight test period. During the flight tests communication was enabled between FTIE and Meteo France by means of IRIDIUM satcom in order to fine tune the trajectory if needed and possible. The flight trials were executed in close cooperation with ATC. In general the optimal season for encountering jet stream-based CAT conditions is during autumn and winter time, while summer time is considered the least promising. Unfortunately, due to delay the project was forced to fly in summer time. During the flight test period high pressure zones were prevalent over W-Europe, resulting in quite poor CAT seeking conditions. During this one-month time period the opportunity to make a CAT flight test was made only on few occasions. In total 11 CAT flights (including the shake-down flight) were made, resulting in a total airborne duration of 31h20m. Only a very few moderate CAT encounters were obtained during these flights. The executed flight trials are shown on a map in Figure 15. Although quite limited, these few CAT events provided interesting results, especially one at the outskirts of the Alps.

Figure 15: Map showing flights made during DELICAT flight test campaign

## 9 DATA POST-PROCESSING AND ANALYSIS

Available data after the 11 flights were on one hand the aircraft sensors data and on the other hand the lidar data. Following aircraft sensors data were time-stamped and recorded on a data logger in ARINC format:

- Inertial Reference System (IRS, 24 parameters),
- Air Data Computer (DADC, 12 parameters),
- Nose boom vanes (2 parameters),
- Fast True Air Temperature probe (TAT, 1 parameter),
- Beam Steering status information (9 parameters).

Lidar data were recorded in files containing the information of 70 000 shots (700 seconds). For each shot, following parameters were recorded:

- GPS time and position,
- relative laser energy,
- parallel signal sampled on 3584 points,
- perpendicular signal sampled on 3584 points,
- high voltage value for parallel and perpendicular PMTs (indicating the gain).

Parallel and perpendicular signals were corrected from the sun noise level, evaluated from measured level before each shot. Lidar range was fixed to 15 km by acquisition system.

### 9.1 Data Filtering

A first-level filtering of the data consisted in identifying areas where the aircraft was flying straight at constant altitude with nominal lidar and beam steering behaviors. Straight flight at constant altitude ensures that aircraft path was actually probed by the lidar. For this purpose, a simultaneous filter on ALD (altitude), ASB (angle of side slip from nose boom), APIRS and ARIRS (angles of roll and pitch from IRS, respectively) was applied. The parameters were averaged over 10s before filtering to remove some of the noise of the sensors.

Figure 15 shows a sample flight with the altitude (a), 10s-averaged angles of yaw, pitch and roll (b, c and d). Areas passing the filters are highlighted in green. Figure 15 (e) shows the vertical acceleration measured by the IRS along with the green plot indicating the areas passing all filters. Finally, plot (f) shows yaw and pitch angles (before averaging) and 4 areas resulting from the filters and the additional requirement that the area duration is larger than 200s. Those areas are identified as usable and numbered. A total of 30 areas are thus selected among all flights. Area 5, for example, experiences some shaking up to ~1.5m/s2 as shown by Figure 15 (e).

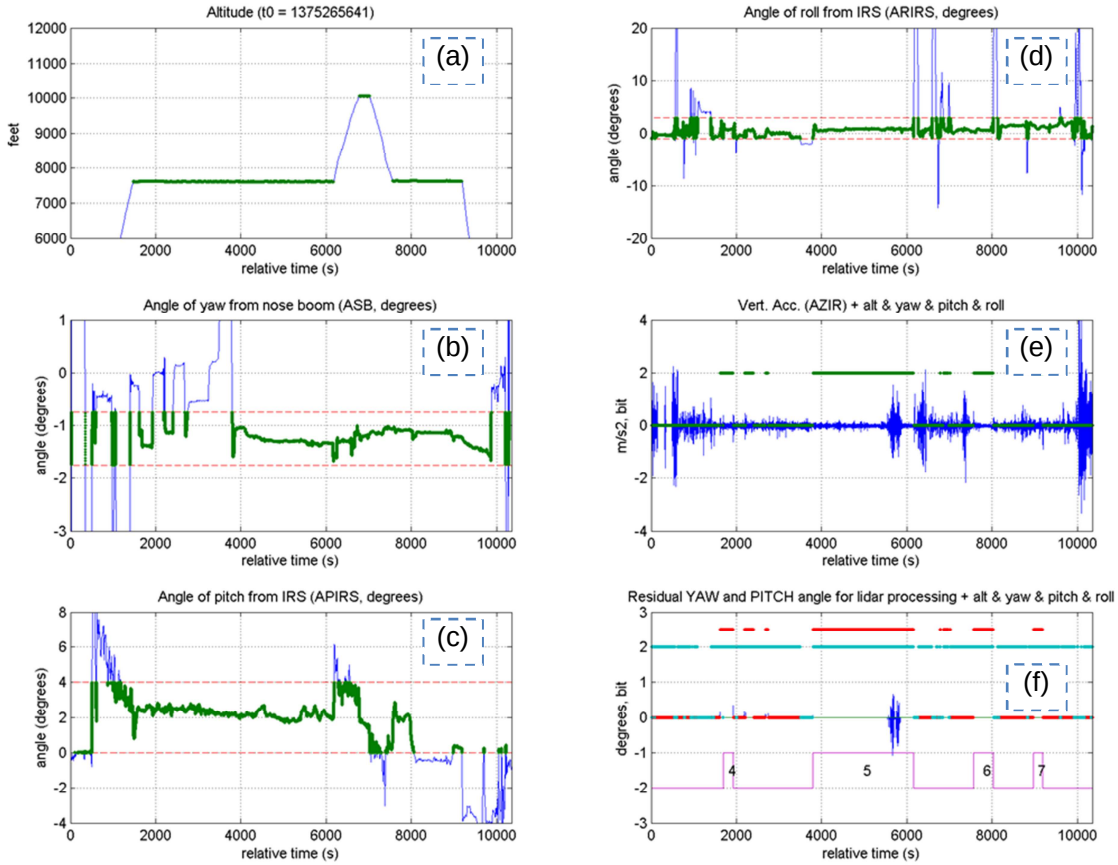


Figure 16: Aircraft sensors 10s-averaged data from flight 4 versus time: altitude (a); angles of yaw (b), pitch (c) and roll (d); vertical acceleration (e). Data passing the filters are highlighted in green. Last plot (f) shows selected areas passing all filters for >200s.

Among the 30 selected areas, 10 are identified as clean from aerosols (using perpendicular channel), among which 4 are considered as containing light CAT encounters and 6 as not containing any CAT encounter. Data were then distributed to partners for further processing. Only Onera preliminary processing results are discussed

## 9.2 Data Pre-processing

Lidar signal is made of parallel and perpendicular polarization channels (relative to emitted light). Perpendicular channel detects the light backscattered by depolarizing aerosols. Parallel channel detects the light backscattered by both the molecules and the non-depolarizing aerosols. Unfortunately, there is no direct way to prove that the signal on parallel channel is in clear air (does only contain molecular signal). But for the considered flight altitude, we make the assumption, based on the mentioned forecast and analysis, that aerosol content of the atmosphere is very small outside of Cirrus clouds (which contain ice crystals at this altitude and thus depolarize).

After a short signal analysis, the first signal processing step is to average the signals (parallel and perpendicular) that have been backscattered from a designated area, taking into account the aircraft speed. The signal is then normalized to remove fluctuations of laser power and lidar alignment noise due to vibrations.

### 9.2.1 Analysis of Lidar Signal

Using an area with no aerosols (pure molecular signal), the lidar parallel signal has been averaged on a long time period to smooth the signal and multiplied by the squared range to correct for the distance dependence (Figure 17 left). In Figure 17 (right) the lidar signal is first corrected from molecular attenuation. This plot shows that the lidar signal is exploitable from 3 km to 15 km. For shorter distances, the signal is saturated or the lidar and the reception field of view do not fully overlap.

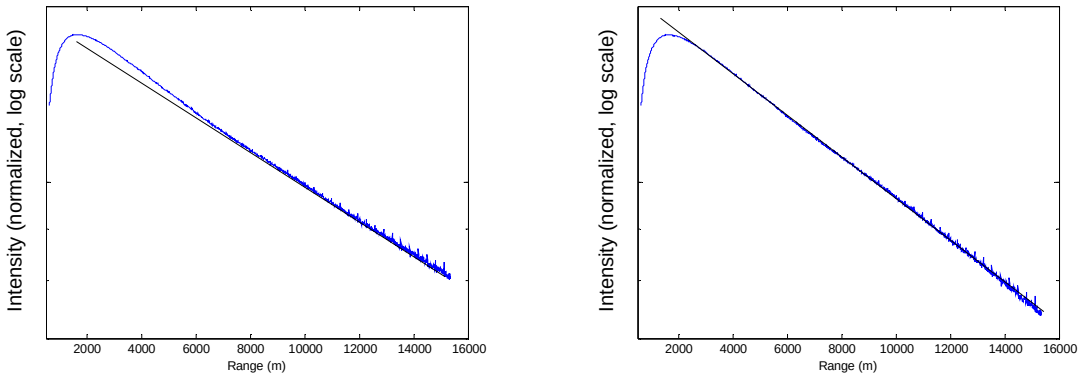


Figure 17.Left: averaged parallel lidar signal multiplied by squared range; Right: averaged lidar parallel lidar signal corrected for molecular attenuation (extinction) and multiplied by squared range.

### 9.2.2 Signal Averaging

This step consists in using all available information to estimate the power reflected from an air volume.

First, an averaging distance Dr is chosen. The sampling distance is 5m: if Dr is n times the sampling distance, n data points will be averaged. The data will be averaged on one shot in slots of length Dr and on successive shots by shifting the slots by the distance traveled by the aircraft between two shots. Figure 18 shows the procedure used to average successive shots that probe the same air volume Dr. In this case, the length Dr is equal to the distance between 2 lidar samples. In shot 1, only the sample 1b is used. In shot 2, a weighted average of samples 2a and 2b is used, according to their overlap with the considered volume. The averaging distance can be limited between Smin (minimum 3 km) and Smax (limited to 15 km: maximum lidar acquisition range). Here Dr was chosen equal to 30m, averaging are made over distances of 500m starting at 3000m up to 14500m.

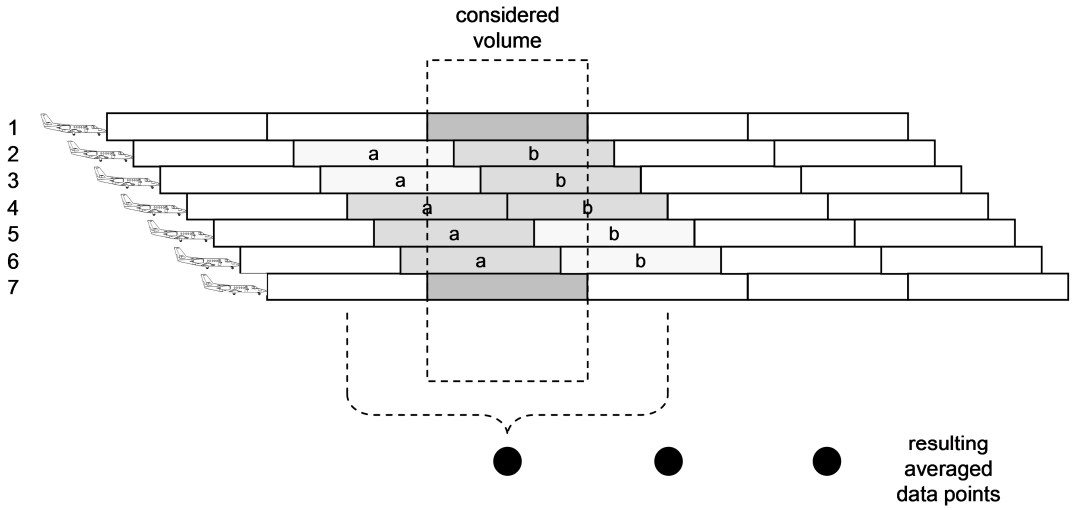


Figure 18 Averaging of various shots in a volume of length Dr

Figure 19 illustrates the averaging procedure in an area containing aerosols: it displays the raw parallel lidar signal multiplied by squared range. Each vertical line is one laser shot. Lidar coupling and laser variations are seen through vertical features whereas variations of the atmospheric backscatter are seen in a slantwise direction due to their motion 'towards the aircraft'.

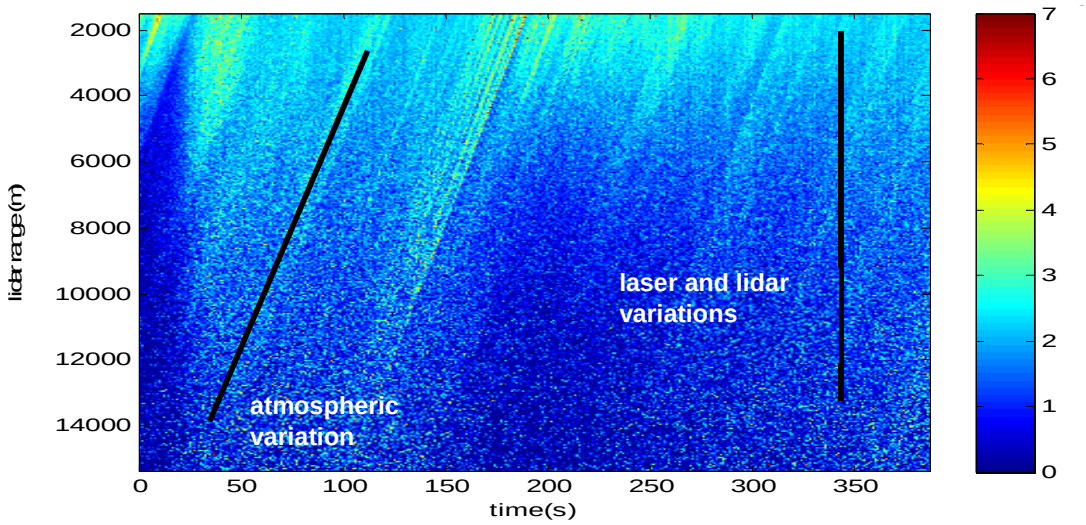


Figure 19 : Lidar parallel signal multiplied by squared range. Each vertical line is a laser shot. Lidar alignment and laser power variations are seen along a horizontal direction whereas atmospheric backscattering variations can be seen in a slantwise direction.

After the averaging step, taking into account the aircraft velocity as detailed above, atmospheric features become visible in the vertical direction and laser/lidar coupling variations become visible slantwise as seen in Figure 20.

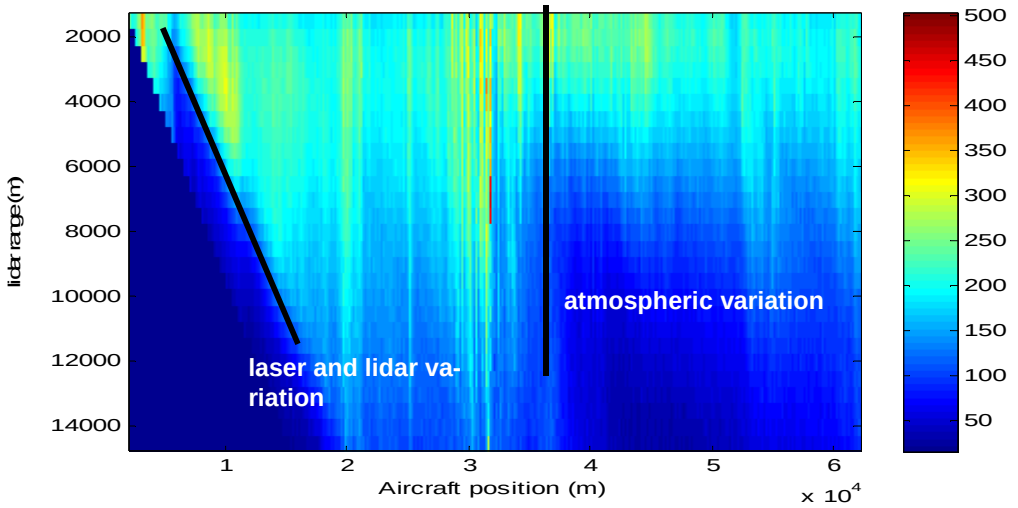


Figure 20 : Averaged signal of Figure 19; atmospheric feature are vertical and laser/lidar variation slantwise.

### 9.2.3 Signal Normalization

The signal is normalized to remove fluctuations of laser power and lidar alignment due to vibrations. Before averaging, for each laser shot, the lidar signal is normalized by the sum of the parallel signal from 3km (end of the saturation) to 15km. The signal normalization removes the slantwise direction modulation (Figure 21).

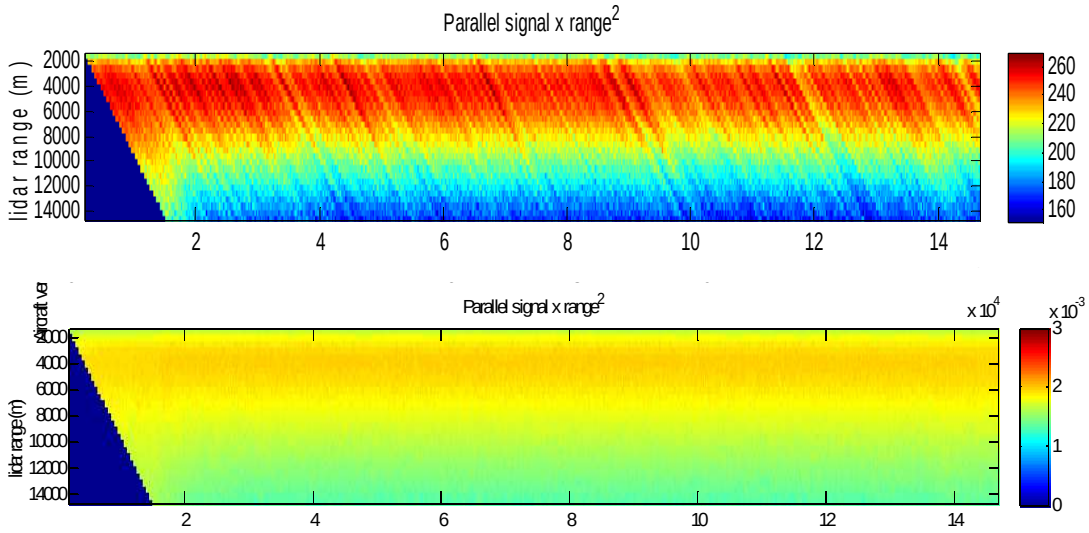


Figure 21: Normalization effect on averaged parallel signal multiplied by the squared range (zone 20 - fligth9). top: without normalization, bottom : with normalization

## 9.3 Sample Results

Figure 22 shows sample pre-processed data for area 5 (see Figure 16). Perpendicular channel seems to indicate that there is no aerosol while parallel channel shows large backscattering. Signal is enhanced by standard deviation processing shown on (c).

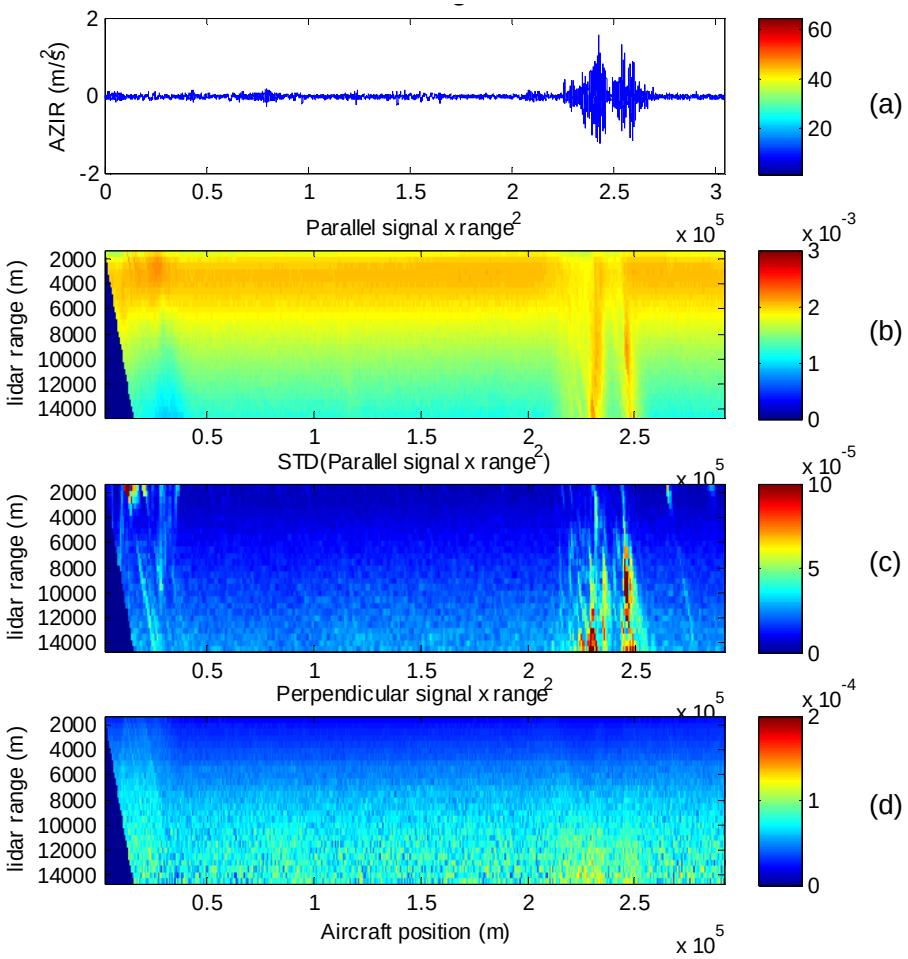


Figure 22: Pre-processed lidar data for area 5: (a) vertical acceleration, (b), parallel signal x range2, (d) perpendicular signal x range2, (c) standard deviation calculated on parallel signal

## 10 CONCLUSIONS

For getting an operational forward looking class 4 UV lidar onboard the aircraft considerable development, modification, installation and certification efforts had to be made. Finally an STC for a LIDAR-modified Citation was obtained. The flight tests were executed successfully, although quite limited number of CAT events could be observed and collected. Currently collected data is still under analysis, preliminary results are promising even though the data sparseness is quite challenging. The first steps towards an airborne sensor for CAT detection at medium distances (>10 km) are made successfully, although the road towards an operational airborne CAT sensor is still long and winding.

## 11 ABBREVIATIONS

| | | |
|---|---|---|
| ATC | - | Air Traffic Control |
| ATM | - | Ait Traffic Management |
| CAA | - | Civil Aviation Authority |
| CAT | - | Clear Air Turbulence |
| CDF | - | Computational Fluid Dynamics |
| DELICAT | - | DEmonstration of LIdar based Clear Air Turbulence detection |
| DLR | - | Deutschen Zentrums für Luft- und Raumfahrt |
| FEM | - | Finite Element Method |

| | | |
|---|---|---|
| IRS | - | Inertial Reference System |
| LIDAR | - | Light Detection And Ranging |
| UV | - | Ultra Violet |

## 12 ACKNOWLEDGEMENTS

The authors would like to thank all colleagues from Thales, DLR, NLR, ONERA, Météo France and ICM that contributed to the preparation and execution of DELICAT flight tests. The flight tests were part of the DELICAT FP7 project, in which a consortium of European companies, research organizations and universities aimed at development of lidar-based CAT detection. The research leading to these results has received funding from the European Union Seventh Framework Programme FP7/2007-2013 under grant agreement n° 233801

## 13 REFERENCES

[1] FAA Advisory Circular AC120-88A, 19/01/2006.

[2] T.N. Venkatesh, J. Mathew, "The problem of clear air turbulence: Changing perspectives in the understanding of the phenomenon ", Sadhana, Vol. 38, Part 4, August 2013, pp. 707–722.

[3] P. Vrancken et al., "Clear air turbulence detection and characterisation in the DELICAT airborne LIDAR project",Proc. Of the 25th ILRS (International Laser radar Conference) St. Petersburg 2010

[4] FP6 FLYSAFE – Final Publishable Report, 25 May 2010

[5] M. Wirth, A. Fix, P. Mahnke, H. Schwarzer, F. Schrandt, and G. Ehret, "The airborne multiwavelength water vapor differential absorption lidar WALES: system design and performance," Applied Physics B: Lasers and Optics, vol. 96, no. 1, pp. 201–213, 2009.